nature astronomy

LETTERS

DOI: 10.1038/s41550-017-0222-1

A nova outburst powered by shocks

Kwan-Lok Li[1*], Brian D. Metzger[2*], Laura Chomiuk[1*], Indrek Vurm[3], Jay Strader[1], Thomas Finzell[1], Andrei M. Beloborodov[2], Thomas Nelson[4], Benjamin J. Shappee[5], Christopher S. Kochanek[6,7], José L. Prieto[8,9], Stella Kafka[10], Thomas W.-S. Holoien[6,7], Todd A. Thompson[6,7], Paul J. Luckas[11] and Hiroshi Itoh[12]

Classical novae are runaway thermonuclear burning events on the surfaces of accreting white dwarfs in close binary star systems, sometimes appearing as new naked-eye sources in the night sky[1]. The standard model of novae predicts that their optical luminosity derives from energy released near the hot white dwarf, which is reprocessed through the ejected material[2–5]. Recent studies using the Fermi Large Area Telescope have shown that many classical novae are accompanied by gigaelectronvolt γ-ray emission[6,7]. This emission likely originates from strong shocks, providing new insights into the properties of nova outflows and allowing them to be used as laboratories for the study of the unknown efficiency of particle acceleration in shocks. Here, we report γ-ray and optical observations of the Milky Way nova ASASSN-16ma, which is among the brightest novae ever detected in γ-rays. The γ-ray and optical light curves show a remarkable correlation, implying that the majority of the optical light comes from reprocessed emission from shocks rather than the white dwarf[8]. The ratio of γ-ray to optical flux in ASASSN-16ma directly constrains the acceleration efficiency of non-thermal particles to be around 0.005, favouring hadronic models for the γ-ray emission[9]. The need to accelerate particles up to energies exceeding 100 gigaelectronvolts provides compelling evidence for magnetic field amplification in the shocks.

ASASSN-16ma (also known as PNV J18205200−2822100, Nova Sgr 2016d or V5856 Sgr) is an optical transient source in the constellation Sagittarius that was discovered by the All Sky Automated Survey for SuperNovae (ASAS-SN; ref. [10]) on 2016 October 25.02 universal time[11]—a corresponding modified Julian day (MJD) of 57686.02—and identified as a normal classical nova with optical spectroscopy[12,13]. The optical light curve of the nova after its discovery showed three distinct phases (Fig. 1). In phase I, the apparent magnitude of the nova, m_V, rose to around 8 mag over two weeks. It then showed a rapid brightening by a factor of around ten over just two days (phase II), reaching a naked-eye peak visual magnitude of 5.4 (MJD 57700). This was followed by a relatively stable decline lasting several weeks (phase III; see Fig. 1 and Methods).

Immediately following the optical peak, our Fermi target-of-opportunity observation detected strong γ-ray emission from the nova with a very high photon flux of $F_{\rm ph,\gamma} \approx 10^{-6}$ photons cm^{-2} s^{-1} (Methods). The γ-ray emission faded rapidly over the next nine days, with only marginal γ-ray detections in the following week. This was among the fastest-evolving γ-ray light curves seen to date from a nova. The optical and γ-ray light curves were tightly correlated, declining at the same rate and showing a simultaneous dip in the emission around MJD 57705 (Fig. 1). The ratio of the γ-ray to optical luminosity (~0.002) remained constant while the γ-rays were detectable (Fig. 1 and Supplementary Information).

The clear correlation between the γ-ray and optical light in ASASSN-16ma led us to reconsider the standard model for nova optical emission[2–5]. Traditionally, the optical emission from novae is attributed to the outwards diffusion of energy released by nuclear burning on the central white dwarf, resulting in emission close to the Eddington luminosity (the critical luminosity at which the outwards radiation force balances inward gravity). The initial rise of the optical light curve is the result of a photosphere expanding at an approximately constant temperature, as much of the released energy goes into expanding the shell. At later times, the observed bolometric luminosity remains approximately constant, with a balance between the receding photosphere and an increasing temperature as the ejecta become optically thin.

However, this standard picture provides no obvious explanation for why the optical emission should track the evolution of the γ-ray emitting shocks, as observed in ASASSN-16ma. Furthermore, we estimate that ASASSN-16ma reached a maximum bolometric luminosity of $L_{\rm tot,opt} \approx 10^{39}\ (d/4.2\,{\rm kpc})^2$ ergs s^{-1} (Methods), where d is the distance of the nova from the Earth, which exceeds the Eddington luminosity by roughly one order of magnitude. Super-Eddington luminosities have also been observed for other novae with well-constrained distances (for example, Nova LMC 1988 #1; ref. [14]) and are a long-standing mystery in the field of nova research.

We instead propose that a large fraction of the optical emission in ASASSN-16ma originates from the same strong shocks responsible for the γ-ray emission[9], providing a natural explanation for the synchronized γ-ray and optical behaviour. This picture capitalizes on the widespread observation that novae undergo abrupt transitions from slower to faster moving outflows[15,16]. In ASASSN-16ma, the structure of the Hα emission line indicates

[1]Department of Physics and Astronomy, Michigan State University, East Lansing, MI 48824, USA. [2]Department of Physics and Columbia Astrophysics Laboratory, Columbia University, New York, NY 10027, USA. [3]Tartu Observatory, Tõravere 61602 Tartumaa, Estonia. [4]Department of Physics and Astronomy, University of Pittsburgh, Pittsburgh, PA 15260, USA. [5]Hubble, Carnegie-Princeton Fellow, Carnegie Observatories, 813 Santa Barbara Street, Pasadena, CA 91101, USA. [6]Department of Astronomy, The Ohio State University, 140 West 18th Avenue, Columbus, OH 43210, USA. [7]Center for Cosmology and Astro-Particle Physics, The Ohio State University, 191 West Woodruff Avenue, Columbus, OH 43210, USA. [8]Núcleo de Astronomía de la Facultad de Ingeniería y Ciencias, Universidad Diego Portales, Avenida Ejército 441, Santiago, Chile. [9]Millennium Institute of Astrophysics, Santiago, Chile. [10]American Association of Variable Star Observers, Cambridge, MA 02138, USA. [11]International Centre for Radio Astronomy Research, The University of Western Australia, 35 Stirling Highway, Crawley, Perth, WA 6009, Australia. [12]Variable Star Observer's League in Japan, 1001-105 Nishiterakata, Hachioji, Tokyo 192-0153, Japan. *e-mail: liliray@pa.msu.edu; bdm2129@columbia.edu; chomiuk@pa.msu.edu

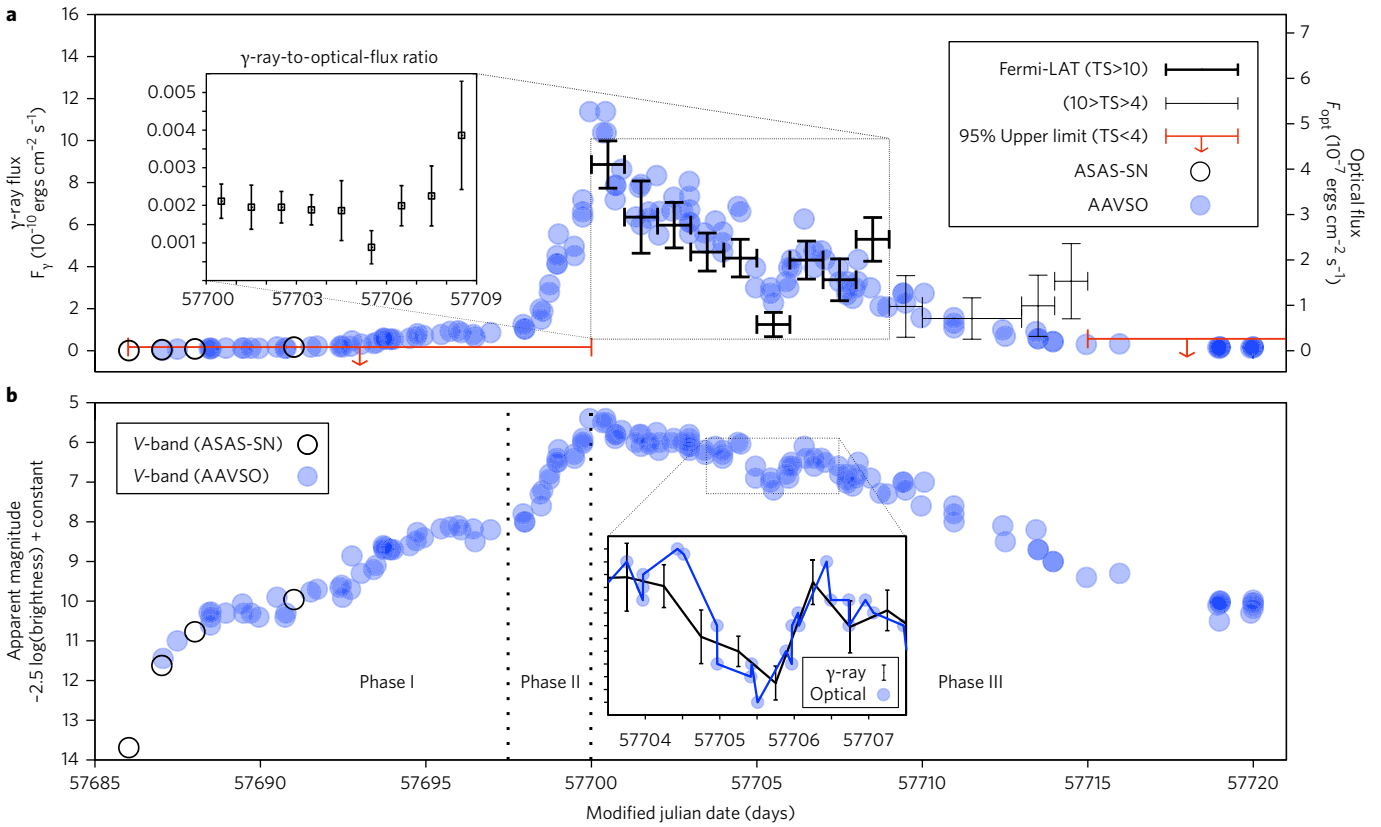

Fig. 1 | Optical and γ-ray light curves track each other. a, γ-ray (black and grey crosses and red arrows) and bolometric (blue and black circles) light curves of ASASSN-16ma in flux units of ergs cm^{-2} s^{-1}, using observations from Fermi-LAT, ASAS-SN and AAVSO. For the Fermi-LAT light curve, most of the data points are daily binned, while some are combined from several daily bins with low detection significance (that is, <2σ). Black and grey colours (with 1σ error bars) represent detection significances larger than ~3σ (that is, TS > 10) and between ~2–3σ (that is, 10 > TS > 4), respectively, while 95% upper limits are indicated by red arrows for bins with a detection significance below ~2σ (that is, TS < 4). Inset: γ-ray-to-optical-flux (luminosity) ratio of ASASSN-16ma, which remained F_γ/F_{opt} ~ 0.002 over the entire γ-ray active period. Error bars show 1σ significance. **b**, *V*-band light curves of the same optical datasets used in **a**, but on a magnitude (logarithmic) scale that clearly shows the three different phases of the optical light curve. Inset: close up of the emission dip at MJD 57705 for γ-rays and optical light, which directly shows the co-variance of the γ-ray and optical emission on timescales as short as 0.5 days.

an acceleration of the nova outflow from $\lesssim$1,100 km s^{-1} in phase I (day 2) to 2,200 km s^{-1} in phase III (day 18–25) (Supplementary Fig. 2). Shortly after the transition, the faster ejecta rapidly expands and collides with the previous slow ejecta. This drives a shock outwards, accelerating particles to relativistic speeds and powering the γ-ray emission[8].

Although we observed the shocks directly by their γ-ray output, most of the total shock power ($L_{sh} \approx 10^{39} \dot{M}_{f4} v_{f2}^2$ ergs s^{-1}, where $\dot{M}_f = 10^{-4} \dot{M}_{f4} M_\odot$ week^{-1} and $v_f = 2{,}000\ v_{f2}$ km s^{-1} are the mass-loss rate and the velocity of the fast ejecta, respectively; Supplementary Information) was radiated as thermal X-rays of temperature $kT \sim 10$ keV. However, these X-rays were strongly attenuated by the dense slow ejecta ahead of the shocks and ultimately escaped as ultraviolet or optical light. This reprocessed emission can dominate the observed optical luminosity of $L_{opt} \sim 10^{38-39}$ ergs s^{-1} in phases II and III (ref. [9]) and is consistent with the X-ray upper limit derived from Swift telescope data around the optical maximum (Methods and Supplementary Information). It is also consistent with the observed constant ratio of the γ-ray and optical luminosities (Fig. 1), assuming the efficiency of relativistic particle acceleration also remains constant in time. In our model, the duration of the optical rise in phase II is the time required for this reprocessed radiation to diffuse through the dense, optically thick, slow outflow. The γ-rays are temporarily attenuated by inelastic electron scattering in the same outflow before their detection at the end of phase II (Supplementary Information).

Key details of the microphysics of the non-thermal emission can be inferred from the γ-ray spectral energy distribution of ASASSN-16ma. Based on a detailed model for the γ-ray emission from radiative shocks[17] (see Supplementary Information for details), we fit the spectral energy distribution in the 100 MeV to 300 GeV energy range to two competing scenarios—the hadronic and leptonic models[6,9,18]. In the hadronic model, accelerated ions strike other ions, producing pions that decay into γ-rays. In the leptonic model, the accelerated electrons emit γ-rays via bremsstrahlung and inverse Compton processes.

Both models give qualitatively reasonable fits (see Fig. 2 and Supplementary Information; for reference only, $\chi^2_\nu = 3.04/6$ and 3.86/6 for the leptonic and hadronic models, respectively). However, consideration of the derived model parameters lends support to the hadronic model. A high shock magnetization (that is, $\epsilon_B \gtrsim 10^{-4}$, where the magnetic field $B = v_{sh}\sqrt{6\pi\epsilon_B\rho}$ and ρ is the upstream density) is required to accelerate particles to energies $\gtrsim$10–100 GeV sufficient to explain the highest energy γ-rays, providing strong evidence for magnetic field amplification at the shock (Supplementary Information). This high magnetization is, however, incompatible with leptonic models, which require $\epsilon_B \lesssim 10^{-6}$ to avoid strong synchrotron cooling losses behind the shock (Supplementary Information). Hadronic models are insensitive to the magnetic field because proton synchrotron cooling is negligible. The hadronic model also naturally predicts a low-energy spectral turnover near the pion rest energy of ~140 MeV, as observed in ASASSN-16ma. However, reproducing

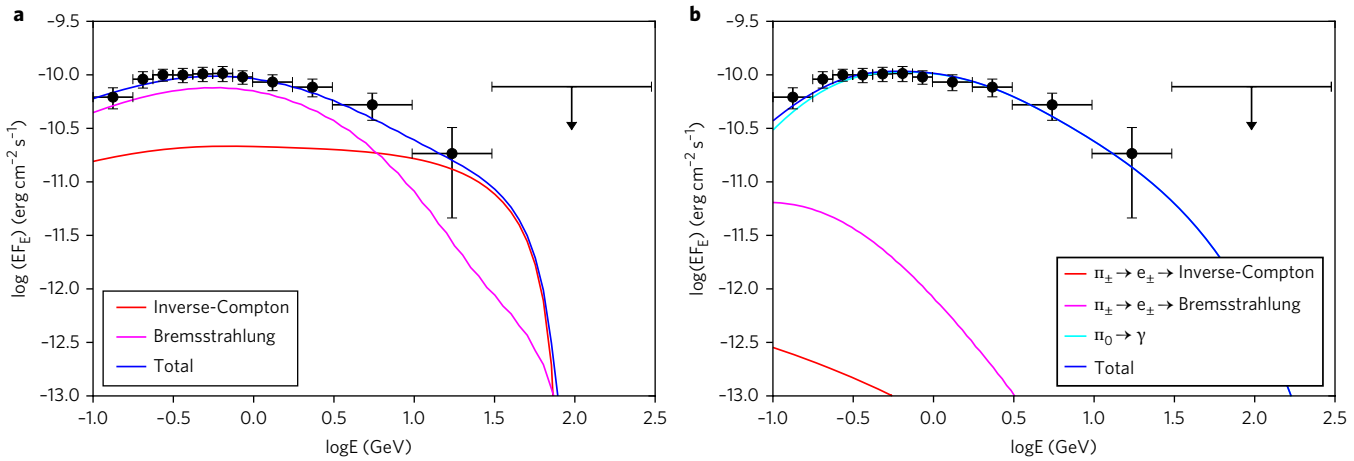

Fig. 2 | γ-ray spectral energy distribution of ASASSN-16ma in two different models. The hadronic model is favoured over the leptonic model based on how the parameters of the model fit to the Fermi γ-ray spectrum. a, Leptonic model: electrons are injected at the shock with the spectrum $dN_e/d\ln\gamma \propto \gamma^{-q}$, where $q = 2$ (equal energy per logarithmic γ interval). **b**, Hadronic model: proton injection spectrum $dN_p/d\ln(\gamma\beta) \propto (\gamma\beta)^{-q}$, where $q = 2.7$. The shock speed and the total shock luminosity are assumed to be 2,000 km s^{-1} and the average optical luminosity, respectively. The radiative processes forming each spectrum are labelled. While both models can describe the data within the statistical errors, the hadronic model is favoured because the leptonic model requires an implausibly high electron acceleration efficiency and cannot produce the >10 GeV γ-ray emission in a self-consistent way (see the main text for details). The reported errors are 1σ uncertainties and the upper limits are at a 95% confidence level.

this same spectral shape in leptonic models requires a lower optical seed radiation field for inverse Compton emission than would be present if the shocks were embedded behind a large column of gas, as our light curve models require for independent reasons. Finally, the inferred proton acceleration efficiency in the hadronic model of $\epsilon_p \approx 5 \times 10^{-3}$ is compatible with the theoretical upper limit from hybrid kinetic shock simulations[19] ($\epsilon_p \lesssim 0.2$; see Supplementary Information for further explanation). In contrast, in leptonic models, a large non-thermal electron acceleration efficiency of $\epsilon_e \approx 2.5 \times 10^{-3}$ is required, in tension with the value $\epsilon_e \approx 10^{-4}$ derived by modelling supernova remnant emission[20] and simulations of particle acceleration in shocks[21]. Taken as a whole, the hadronic model is favoured over the leptonic one.

We examined the available Fermi Large Area Telescope (Fermi-LAT) γ-ray and optical data of the other five Fermi-detected classical novae[6,7,22] to explore further evidence for the correlation between optical and γ-ray luminosity clearly observed in ASASSN-16ma (V959 Mon 2012 and V407 Lup 2016 were excluded from the analysis because no useful optical data were taken for V959 Mon 2012 when the γ-ray counterpart was bright[6] and V407 Lup 2016 was just marginally detected with a significance of 4.4σ; ref. [23]). The two γ-ray classical novae V339 Del and V5855 Sgr exhibited marginally correlated optical and γ-ray light curves with a significance of around 2σ, suggesting that ASASSN-16ma may not be an orphan (Supplementary Fig. 6). If the particle acceleration efficiency in ASASSN-16ma is representative of all γ-ray novae, then given the γ-ray-to-optical-luminosity ratios in the other novae[6,7,9], we can conclude that a significant fraction of the optical emission in these other events must also be powered by shocks. In V1369 Cen and V5668 Sgr, weak evidence may exist to support the claim insofar as the γ-ray emission in both events was detected only during epochs of bright optical emission (that is, $m_V \lesssim 5$ mag for V1369 Cen and $\lesssim 6$ mag for V5668 Sgr; ref. [7]). In addition, the γ-ray emission in most other novae begins near the first optical peak[6,7], as expected from shocks developing between the fast and slow flows. Prompt γ-ray observations of future galactic novae will allow the universality of this model to be tested.

Through γ-ray and optical observations of ASASSN-16ma, we have shown that nova optical emission can be indirectly powered by shocks below the photosphere, thus verifying a prediction first made by refs [8,9]. This discovery challenges the standard model that most ultraviolet or optical emission in novae is the result of outwards diffusion of the radiation from the white dwarf[24]. In addition, it provides a solution for the long-standing mystery of why many novae exceed the Eddington luminosity[25]: shock-driven emission, unlike the hydrostatic atmosphere of the white dwarf, obeys no such luminosity limit (Supplementary Information). Our results also confirm how the dense nova ejecta serve as an effective 'calorimeter' for relativistic particles[9]: the power and acceleration efficiency of the shock are measured directly from the ultraviolet or optical and γ-ray luminosities, respectively (Supplementary Information). Given the conditions at the shock required to explain the observed luminosities, coupled with the need to accelerate particles to energies exceeding 100 GeV, we find strong evidence for magnetic field amplification at the shocks (Supplementary Information)—a topic of active debate in other astrophysical settings such as supernova remnants[26].

Methods

ASAS-SN discovery of ASASSN-16ma. ASASSN-16ma was detected at $m_V = 13.69 \pm 0.02$ mag by the ASAS-SN on 2016 October 25.02 universal time using the quadruple 14 cm 'Cassius' telescope at the Cerro Tololo Inter-American Observatory in Chile[11]. A rising light curve (Fig. 1) was revealed by the subsequent observations with m_V magnitudes of 11.62 ± 0.01 mag (day 1), 10.77 ± 0.01 mag (day 2) and 9.96 ± 0.01 mag (day 5). No object could be detected at the nova position in the previous ASAS-SN observations beginning in March 2016, and the final pre-discovery image taken on 2016 October 20.04 placed a limiting magnitude of $m_V > 17.3$ mag on the progenitor.

American Association of Variable Star Observers (AAVSO): photometry, temperature and distance. AAVSO is an astronomical association of observers—amateur and professional—that provides optical photometric observations of variable sources. We downloaded the photometric datasets from the AAVSO International Database, including both visual estimates of magnitudes and those quantified by CCD photometry. Most of the AAVSO data are visual magnitudes, which for experienced observers are consistent with standard V magnitudes. Some epochs have CCD photometry, including multi-band measurements in BV, which we used to estimate the nova temperature below. The photometry presented here spans the date range MJD 57687–57719. Unless otherwise mentioned, a galactic reddening of $E(B-V) = 0.34$ mag ($A_V = 1.06$ mag with $R_V = 3.1$) was assumed[27].

From the V-band light curve, the optical evolution can be divided into three major phases, namely phases I, II and III (Fig. 1). In phase I (from about MJD 57687–57697), the optical emission rose at a mean rate of $\dot{m}_V \approx -0.3$ mag day^{-1}, but with two apparent plateaus in the light curve during which the

optical brightness did not change for two to three days. In phase II (from about MJD 57698–57700), the nova brightened rapidly by $\dot{m}_V \approx -1.3$ mag day^{-1} and the emission reached a maximum of $m_V = 5.4$ mag (or $m_{V,0} = 4.3$ mag corrected for extinction) on MJD 57700. In phase III, the emission started to decrease from the peak at a rate of $\dot{m}_V \approx 0.2$ mag day^{-1} until the end of the dataset. The only clear short-term variability was a $\Delta m_V \approx 1$ mag dip around MJD 57705.5, which lasted for one to two days. This dip feature was also present with a similar profile in the Fermi-LAT MeV/GeV light curve (Fig. 1). We note that the ANS Collaboration also monitored the nova using a 40 cm robotic telescope and all the aforementioned optical features also appear in the ANS light curve[28].

Colour temperatures (T_c) of the nova photosphere over time were estimated with the night sets of *B*- and *V*-band data. While the earliest dataset (MJD 57687, about 1 day after the ASAS-SN discovery) showed a relatively blue colour of $(B-V)_0 = -0.02$ mag (extinction corrected; equivalent to a colour temperature of $T_c = 10{,}300$ K; ref. [29]), the subsequent colours levelled off in the range of $(B-V)_0 = 0.16$–0.27 mag ($T_c = 7{,}200$–$8{,}100$ K) with an average $(B-V)_0 = 0.21$ mag ($T_c = 7{,}700$ K). The latest colour on MJD 57704.5 went redder to $(B-V)_0 = 0.57$ mag ($T_c = 5{,}500$ K; see Supplementary Table 1). The observed colour near the optical peak, $(B-V)_0^{\max} = 0.24$, was close to that typically observed for novae[30], showing that the adopted extinction was reasonable (Supplementary Table 1).

The decay rate in phase III was used to estimate the nova distance through the maximum magnitude–rate of decline (MMRD) relationship. We used the linear empirical equation of *V*-band absolute magnitude at maximum (M_V) and the time (in days) needed to decline two magnitudes from the peak (t_2), of

$$M_V = (-11.32 \pm 0.44) + (2.55 \pm 0.32)\log t_2, \quad (1)$$

from Downes et al.[31] to estimate an absolute magnitude of $M_V = -8.8 \pm 0.5$ mag for $t_2 = 10$ days, implying a distance of $d = 4.2^{+1.2}_{-0.9}$ kpc, which was roughly consistent with $d \approx 6.4$ kpc estimated by Munari et al.[28]. We also checked the result with the non-linear version[31],

$$M_V = -8.02 - 1.23 \arctan\left[\frac{1.32 - \log t_2}{0.23}\right], \quad (2)$$

which gives a consistent result of $M_V = -9.2$ mag and $d = 5.1$ kpc. Despite the large uncertainties and the uncertain reliability of the MMRD method[32], many of our main results, such as the acceleration efficiency inferred from the γ-ray-to-optical-flux ratio, are not sensitive to the distance. We adopted the linear MMRD distance of $d = 4.2$ kpc as a reference distance in our analysis, but caution that the uncertainties in the distance do not include systematic uncertainties in the MMRD. For example, Kasliwal et al.[32] found that some novae with $t_2 \sim 10$ days (the observed value for ASASSN-16ma) were up to 2 mag fainter than predicted by the MMRD, which would imply a distance of only 1.7 kpc. At this short distance, the inferred luminosity could be consistent with the Eddington luminosity, depending on the mass of the white dwarf. Besides the MMRD technique, we assumed the peak brightness of ASASSN-16ma to be equal to the Eddington luminosity for a 1 $M_\odot$ white dwarf and $M_V \approx -8.7$, the mean absolute magnitude of the galactic novae at peak[33], which infer distances of $d = 1.4$ kpc and 4.1 kpc, respectively. The later value is very close to our reference distance of 4.2 kpc.

Variable Star NETwork (VSNET): photometry and temperature. VSNET is a collaboration whose members share their observational results (mainly in optical) of variable stars and new transients, including ASASSN-16ma. Supplementary Table 1 presents the VSNET photometric measurements and the inferred colour temperatures (using the same approach as for the AAVSO data), which are mostly consistent with the AAVSO result.

Astronomical Ring for Access to Spectroscopy (ARAS): temperature and Hα line. Despite its brightness, only limited optical spectroscopy of ASASSN-16ma was possible owing to its discovery close to the Sun. Spectroscopy was undertaken by Luckas over eight epochs from 27 October to 18 November 2016 (universal time) and submitted to the ARAS database for distribution. The observations used an Alpy 600 spectrograph with a low-resolution grism, mounted on a 36 cm telescope. The exposure times varied from around 1 h (immediately after discovery) to 10 min (near the optical peak). The observations were reduced in the standard manner, with wavelength calibration using a neon arc lamp. The resulting spectra had a resolution of about 11.4 Å full width at half maximum (520 km s^{-1}) in the region of Hα.

After extinction corrections, we fit a blackbody model to the five spectra with clear photospheric continuum emission (at late times, the spectra were consistent with only line emission). The inferred temperatures were consistent with those extracted from the AAVSO and VSNET photometry (Supplementary Table 1). In addition, we detected the Hα emission line in all eight epochs of spectroscopy, with the profile changing from an unresolved narrow line with a pair of $\pm 1{,}100$ km s^{-1} wings to a P Cygni profile, and finally a broad line with wings extending to $\pm 2{,}200$ km s^{-1} (Supplementary Fig. 2).

Pre-nova observations. While a faint near-infrared source detected in 2010 by the Visible and Infrared Survey Telescope for Astronomy Variables in the Via Lactea survey was first proposed to be the progenitor[34], it has been shown that this source is 1.6 arcseconds from the nova location and cannot be the true progenitor[35]. In fact, no progenitor source has yet been detected to $m_I > 22$ mag, constrained by the Optical Gravitational Lensing Experiment deep template image[35]. Taking the extinction $A_I = 0.63$ mag and the MMRD distance $d = 4.2$ kpc into account, the absolute magnitude of the progenitor is $M_{I,0} > 8.3$ mag, indicating that the binary companion of the nova system is likely a main-sequence star, probably an M-type dwarf.

Bolometric correction of the optical light curve. For a comprehensive comparison with the Fermi γ-ray data, bolometric corrections[36] (BC) were estimated for 16 epochs (that is, MJD 57687.0–57704.5) based on the temperatures inferred from the AAVSO and VSNET photometry and the ARAS spectra. Individual corrections were estimated using: (1) the first measurement of BC = −0.38 mag for epochs before MJD 57687.0; (2) interpolation of the measurements for epochs between MJD 57687.0 and 57704.5 (that is, BC = −0.11 to −0.19 mag); or (3) the last measurement of BC = −0.19 mag for the later epochs. Although the adopted BC values may not be ideal for all epochs (that is, early phase I and late phase III), the corrections are sufficient for our purposes.

Fermi-LAT. We used Fermi-LAT Pass 8 observations taken from 25 October 2016 (mission elapsed time: 499,046,404 s; the ASAS-SN discovery date) to 28 November 2016 (mission elapsed time: 502,043,986 s) within a circular region of interest of 20° radius around the nova optical position at α(J2000) = 18 h 20 m 52.12 s, δ(J2000) = −28° 22′ 13.52″ (ref. [11]). For nearly the entire time (that is, from 25 October 2016 to 16 November 2016), Fermi-LAT was operated in a target-of-opportunity galactic centre-biased survey mode for the nova field. This mode was serendipitously active from the initial discovery of ASASSN-16ma, as the target-of-opportunity observations were originally triggered for another nearby classical nova (V5855 Sgr; observation number: 090603-1-1). Fermi-LAT resumed observations in its regular survey mode after 16 November 2016. The period of highest sensitivity observations covered nearly all of phases I and II and the first eight days of phase III, ending on MJD 57708.

Fermi Science Tools (version v10r0p5; https://fermi.gsfc.nasa.gov/ssc/data/analysis/software/) software was used to analyse the LAT data (100 MeV–300 GeV) by following the online data analysis threads of the Fermi Science Support Center. We first constructed an emission model of the event data by considering all catalogued sources within 30° from the nova (that is, the region of interest plus an extra 10°) in the LAT 4-Year Point Source Catalog (3FGL; ref. [37]) with the diffuse background components of galactic diffuse emission (gll_iem_v06) and extragalactic isotropic diffuse emission (iso_P8R2_SOURCE_V6_v06). As the nearby sources were too faint to significantly affect the result (in fact, ASASSN-16ma was the dominant source within 5° of the field during the time of interest), we only allowed the intensities (normalization) of the two closest 3FGL sources (that is, 3FGL J1816.2–2726 and 3FGL J1823.7–3019; 3° within the nova) to vary and fixed all the other spectral parameters of the 3FGL sources in the model file. In addition, we noticed from our trial runs that the best-fit extragalactic isotropic diffuse emission would drop to 60% of the regular level if it was not fixed. Therefore, we also fixed its normalization to unity (that is, the default value) to avoid overestimating the γ-ray flux of ASASSN-16ma.

An initial analysis was performed with the task 'like_lc' (version 1.72; developed by R. Corbet), which is a python script for generating LAT light curves using the unbinned likelihood analysis method. With a simple power-law model fit to the γ-ray spectrum ($dN/dE \propto E^{-\Gamma_\gamma}$ with a fixed $\Gamma_\gamma = 2.1$, the best-fit value found by the binned likelihood analysis described later in this section), we extracted a one day binned light curve in which significant γ-ray emission was detected starting from 8 November 2016 (MJD 57700, also the date of the optical peak) with a daily test statistic (TS) = 200 (equivalent to a detection significance of $\sqrt{\mathrm{TS}} \approx 14\sigma$) and a photon flux of $F_{\mathrm{ph},\gamma} = (1.04 \pm 0.13) \times 10^{-6}$ photons cm^{-2} s^{-1} (100 MeV–300 GeV). The γ-ray flux then decreased with $F_{\mathrm{ph},\gamma} \propto (t - t_0)^{-0.33 \pm 0.04}$ (where t_0 = MJD 57700, the γ-ray onset) and dropped below the Fermi-LAT 3σ detection limits (that is, TS < 10) on 17 November 2016. After this, only weak γ-ray signals with around 2σ were occasionally detected. We therefore conclude that the detectable γ-ray emission lasted for 9–15 days in total (Fig. 1 and Supplementary Table 2). In addition to the overall trend of decreasing γ-ray flux, we clearly detected a dip around MJD 57705.5. To check the spectral index of the dip, we tried to free the daily photon index, but the dip duration was too short for meaningful constraints. However, a general softening trend over the whole γ-ray active phase was marginally observed (Supplementary Fig. 5). This could support a weakening attenuation of the γ-ray emission as the system evolves (see Supplementary Information).

Besides the likelihood light curve, a 0.5 day binned light curve extracted by aperture photometry using the task 'aperture' (version 1.53; developed by R. Corbet) and a circular region of 1° radius was examined. Despite the non-subtracted background, the aperture light curve was mostly consistent with the likelihood one, with the same dip feature and a similar decline. With a finer resolution, the aperture light curve confirmed that the γ-ray onset started with the optical peak and also showed that the dip profiles in optical and γ-rays were very similar to each other in structure (Fig. 1).

Using all the Fermi-LAT observations with daily TS > 10, we performed a stacked spectral analysis using the binned likelihood method. For the same region

of interest, emission model and energy range, we modelled the data with a simple power law resulting in TS = 635, $\Gamma_\gamma = 2.11 \pm 0.05$ and $F_{ph,\gamma} = (5.9 \pm 0.5) \times 10^{-7}$ photons cm^{-2} s^{-1} (errors are statistical only). We found that the fit could be improved significantly (~3σ using the likelihood ratio test) by introducing an exponential cutoff ($dN/dE \propto E^{-s} \exp(-E/E_c)$, where E_c is the cutoff energy), to find TS = 644, $s = 1.86 \pm 0.11$, $E_c = 5.9 \pm 2.6$ GeV and $F_{ph,\gamma} = (5.4 \pm 0.5) \times 10^{-7}$ photons cm^{-2} s^{-1} (Supplementary Table 3). We also carried out a time-resolved spectral analysis before and after the dip, which showed the spectrum getting softer from $\Gamma_\gamma = 2.05 \pm 0.06$ to 2.22 ± 0.10, confirming the softening trend seen in the unbinned likelihood light curve. Adding an exponential energy cutoff did not significantly improve the after-dip spectral fit, in contrast with the before-dip and the overall fits (Supplementary Table 3). This could have been caused by an unknown intrinsic spectral change or, more likely, the lower signal-to-noise ratio of the after-dip data. To produce a spectral energy distribution for detailed modelling, we also manually split the data into 12 energy bins and ran binned likelihood analyses (Fig. 2; see Supplementary Information for details of the spectral model).

We refined the position of the γ-ray source using the task 'gtfindsrc' with the region of interest decreased from 20° to 10° to save computational time. The optimized coordinates were α(J2000) = 18 h 20 m 57.87 s, δ(J2000) = −28° 21′ 40.9″ (95% error circle radius: 2.7′). The nova was 1.4′ from this position and hence well inside the Fermi error circle.

γ-ray and optical correlation in ASASSN-16ma. To estimate the significance of the correlation of ASASSN-16ma, we computed the Pearson correlation coefficients of the AAVSO *V*-band light curve with; (1) the Fermi aperture light curves (r_a); and (2) the Fermi-LAT likelihood light curves (r_l). Since the γ-ray and optical light curves were sampled differently, the optical data were linearly interpolated to pair up with the γ-ray data. For the Fermi-LAT data with daily TS > 10, the Pearson coefficients were $r_a = 0.75$ (16 degrees of freedom) and $r_l = 0.86$ (7 degrees of freedom), which correspond to two-tailed *P* values of 3.7×10^{-4} (3.6σ) and 3.1×10^{-3} (3σ), respectively. Note that the above significance values are very conservative, as the γ-ray observations with low detection significance (TS < 10) and the temporal coincidence of the γ-ray and the optical peaks were not considered.

Peak and dip offsets between the γ-rays and optical light curves. Owing to the continuous monitoring by Fermi, the γ-ray peak was well constrained on MJD $57{,}700.05 \pm 0.05$ by a 0.1 day binned light curve and the dip minimum was well constrained on MJD 57705.75 ± 0.25 by a 0.5 day binned light curve. For the AAVSO light curve, owing to the relatively low sampling rate, the optical peak and dip minimum fell within wide ranges of MJD 57699.95–57700.34 (ref. [28]) and MJD 57705.50–57705.96, respectively. After subtractions, the offsets (positive for a γ-ray delay) were from −8 to +4 h and from −11 to +12 h for the peak and dip, respectively.

Swift X-ray telescope. During the γ-ray active phase, the visibility of ASASSN-16ma was limited for all satellite X-ray observatories due to the Sun angle constraint. Thus, only one short (2 ks) X-ray observation was taken for ASASSN-16ma by the Swift X-ray telescope in the Windowed Timing mode on MJD 57701 (9 November 2016; one day after the γ-ray onset). As the data were very noisy below 1 keV, only the 1–10 keV band was used to search for the X-ray counterpart. At a 3σ threshold, ASASSN-16ma was not detected with a 95% upper limit[38] of $< 4 \times 10^{-13}$ ergs cm^{-2} s^{-1} (assuming an absorbed power-law with $\Gamma_X = 2$ and foreground absorption[39] of $N_H = 1.33 \times 10^{21}$ cm^{-2}; absorption corrected). This is consistent with a 1–10 keV upper limit of $L_X \lesssim 10^{33}$ ergs s^{-1} at the adopted distance. About five months later, we requested another 2.4 ks Swift X-ray telescope observation, taken in the Photon Counting mode on 23 March 2017 (MJD 57835). The nova was still undetected with an upper limit[40] of $< 2 \times 10^{-13}$ ergs cm^{-2} s^{-1} (or 4×10^{32} ergs s^{-1}; 0.3–10 keV).

Data availability. The data that support the findings of this study are available from the LAT Data Server (https://fermi.gsfc.nasa.gov/ssc/), AAVSO data archive (https://www.aavso.org/data-download), VSNET official page (http://www.kusastro.kyoto-u.ac.jp/vsnet/) and ARAS spectral database (http://www.astrosurf.com/aras/Aras_DataBase/DataBase.htm).

Received: 19 June 2017; Accepted: 13 July 2017;

References

1. Warner, B. *Cataclysmic Variable Stars* (Cambridge Univ. Press, Cambridge, 2003).
2. Gallagher, J. S. & Starrfield, S. Theory and observations of classical novae. *Ann. Rev. Astron. Astrophys.* **16**, 171–214 (1978).
3. Kato, M. Optically thick winds and nova outbursts. *Publ. Astron. Soc. Jpn* **35**, 507–519 (1983).
4. Gehrz, R. D., Truran, J. W., Williams, R. E. & Starrfield, S. Nucleosynthesis in classical novae and its contribution to the interstellar medium. *Publ. Astron. Soc. Pac.* **110**, 3–26 (1998).
5. Bode, M. F. & Evans, A. *Classical Novae* (Cambridge Univ. Press, Cambridge, 2012).
6. Ackermann, M. et al. Fermi establishes classical novae as a distinct class of gamma-ray sources. *Science* **345**, 554–558 (2014).
7. Cheung, C. C. et al. Fermi-LAT gamma-ray detections of classical novae V1369 Centauri 2013 and V5668 Sagittarii 2015. *Astrophys. J.* **826**, 142 (2016).
8. Metzger, B. D. et al. Shocks in nova outflows—I. Thermal emission. *Mon. Not. R. Astron. Soc.* **442**, 713–731 (2014).
9. Metzger, B. D. et al. Gamma-ray novae as probes of relativistic particle acceleration at non-relativistic shocks. *Mon. Not. R. Astron. Soc.* **450**, 2739–2748 (2015).
10. Shappee, B. J. et al. The man behind the curtain: X-rays drive the UV through NIR variability in the 2013 active galactic nucleus outburst in NGC 2617. *Astrophys. J.* **788**, 48 (2014).
11. Stanek, K. Z. et al. ASAS-SN discovery of a likely galactic nova ASASSN-16ma on the rise. *The Astronomer's Telegram* **9669** (2016).
12. Luckas, P. Spectroscopic confirmation of ASASSN-16ma as a classical nova in the Fe-curtain stage. *The Astronomer's Telegram* **9678** (2016).
13. Rudy, R. J., Crawford, K. B. & Russell, R. W. Optical and infrared spectral features of the galactic nova ASASSN-16ma (PNV J18205200-2822100). *The Astronomer's Telegram* **9849** (2016).
14. Schwarz, G. J. et al. A multiwavelength study of the early evolution of the classical nova LMC 1988 1. *Mon. Not. R. Astron. Soc.* **300**, 931–944 (1998).
15. Friedjung, M. The physics of the nova phenomenon, III. *Mon. Not. R. Astron. Soc.* **132**, 317–336 (1966).
16. Kato, M. & Hachisu, I. Effects of a companion star on slow nova outbursts: transition from static to wind evolutions. *Astrophys. J.* **743**, 157 (2011).
17. Vurm, I. & Metzger, B. D. High-energy emission from non-relativistic radiative shocks: application to gamma-ray novae. Preprint at https://arxiv.org/abs/1611.04532 (2016).
18. Martin, P. & Dubus, G. Particle acceleration and non-thermal emission during the V407 Cygni nova outburst. *Astron. Astrophys.* **551**, A37 (2013).
19. Caprioli, D. & Spitkovsky, A. Simulations of ion acceleration at non-relativistic shocks. I. Acceleration efficiency. *Astrophys. J.* **783**, 91 (2014).
20. Morlino, G. & Caprioli, D. Strong evidence for hadron acceleration in Tycho's supernova remnant. *Astron. Astrophys.* **538**, A81 (2012).
21. Park, J., Caprioli, D. & Spitkovsky, A. Simultaneous acceleration of protons and electrons at nonrelativistic quasiparallel collisionless shocks. *Phys. Rev. Lett.* **114**, 085003 (2015).
22. Li, K.-L. & Chomiuk, L. Fermi-LAT detection of the galactic nova TCP J18102829-2729590. *The Astronomer's Telegram* **9699** (2016).
23. Cheung, C. C., Jean, P., Shore, S. N. & Fermi Large Area Telescope Collaboration. Fermi-LAT gamma-ray observations of nova Lupus 2016 (ASASSN-16kt). *The Astronomer's Telegram* **9594** (2016).
24. Yaron, O., Prialnik, D., Shara, M. M. & Kovetz, A. An extended grid of nova models. II. The parameter space of nova outbursts. *Astrophys. J.* **623**, 398–410 (2005).
25. Duerbeck, H. W. Light curve types, absolute magnitudes, and physical properties of galactic novae. *Publ. Astron. Soc. Pac.* **93**, 165–175 (1981).
26. Ressler, S. M. et al. Magnetic field amplification in the thin X-ray rims of SN 1006. *Astrophys. J.* **790**, 85 (2014).
27. Schlafly, E. F. & Finkbeiner, D. P. Measuring reddening with Sloan Digital Sky Survey stellar spectra and recalibrating SFD. *Astrophys. J.* **737**, 103 (2011).
28. Munari, U., Hambsch, F. J. & Frigo, A. Photometric evolution of seven recent novae and the double component characterizing the lightcurve of those emitting in gamma rays. *Mon. Not. R. Astron. Soc.* **469**, 4341–4358 (2017).
29. Kitchin, C. R. *Astrophysical Techniques*. 5th edn (CRC Press, Florida, 2009).
30. Van den Bergh, S. & Younger, P. F. UBV photometry of novae. *Astron. Astrophys. Suppl. Ser.* **70**, 125–140 (1987).
31. Downes, R. A. & Duerbeck, H. W. Optical imaging of nova shells and the maximum magnitude–rate of decline relationship. *Astron. J.* **120**, 2007–2037 (2000).
32. Kasliwal, M. M. et al. Discovery of a new photometric sub-class of faint and fast classical novae. *Astrophys. J.* **735**, 94 (2011).
33. Munari, U. Classical and recurrent novae. *JAAVSO* **40**, 582–597 (2012).
34. Saito, R. K., Minniti, D., Catelan, M. & Angeloni, R. The likely progenitor of nova ASASSN-16ma. *The Astronomer's Telegram* **9680** (2016).
35. Mroz, P., Udalski, A. & Pietrukowicz, P. OGLE-IV pre-discovery observations of two recent galactic novae. *The Astronomer's Telegram* **9683** (2016).
36. Weidemann, V. & Bues, I. On the scale of bolometric corrections. *Zeitschrift für Astrophysik* **67**, 415–419 (1967).
37. Acero, F. et al. Fermi large area telescope third source catalog. *Astrophys. J. Suppl.* **218**, 23 (2015).
38. Kraft, R. P., Burrows, D. N. & Nousek, J. A. Determination of confidence limits for experiments with low numbers of counts. *Astrophys. J.* **374**, 344–355 (1991).

39. Kalberla, P. M. W. et al. The Leiden/Argentine/Bonn (LAB) survey of Galactic HI. Final data release of the combined LDS and IAR surveys with improved stray-radiation corrections. *Astron. Astrophys.* **440**, 775–782 (2005).
40. Evans, P. A. et al. An online repository of Swift/XRT light curves of γ-ray bursts. *Astron. Astrophys.* **469**, 379–385 (2007).

Acknowledgements

We acknowledge the variable star observations from the AAVSO International Database contributed by observers worldwide and used in this research. We thank the Fermi Science Support Center, supported by the Flight Operations Team, for scheduling the Fermi target-of-opportunity observations. We also acknowledge the use of public data from the Fermi and Swift data archives. We thank Las Cumbres Observatory and its staff for their continued support of ASAS-SN. ASAS-SN is funded in part by the Gordon and Betty Moore Foundation through grant GBMF5490 to the Ohio State University. ASAS-SN is supported by National Science Foundation grant AST-1515927. Development of ASAS-SN has been supported by National Science Foundation grant AST-0908816, the Center for Cosmology and Astro Particle Physics at the Ohio State University, the Mt. Cuba Astronomical Foundation and G. Skestos. We also acknowledge useful discussions with J. Linford, A. Mioduszewski, K. Mukai, J. Sokoloski, K. Stanek and J. Weston, which greatly improved the quality of the paper. This work was partially supported by Fermi GI grant NNX14AQ36G. I.V. acknowledges support from the Estonian Research Council grant PUT1112. J.S. acknowledges support from the Packard Foundation. L.C. acknowledges a Cottrell Scholar Award from the Research Corporation for Science Advancement. B.J.S. is supported by the National Aeronautics and Space Administration through Hubble Fellowship grant HST-HF-51348.001 awarded by the Space Telescope Science Institute, which is operated by the Association of Universities for Research in Astronomy for the National Aeronautics and Space Administration, under contract NAS 5-26555. T.W.-S.H. is supported by the Department of Energy's Computational Science Graduate Fellowship, grant number DE-FG02-97ER25308. C.S.K. and T.W.-S.H. are supported by National Science Foundation grants AST-1515876 and AST-1515927.

Author contributions

K.-L.L., B.D.M., L.C., I.V. and J.S. wrote the paper. B.J.S, C.S.K., J.L.P., T.W.-S.H. and T.A.T., on behalf of the ASAS-SN team, discovered ASASSN-16ma and provided the ASAS-SN data. S.K., the director of AAVSO, provided the AAVSO light curves through the AAVSO International Database. P.J.L. observed and provided the ARAS spectroscopic data. H.I., on behalf of the VSNET team, provided useful photometric data. L.C., K.-L.L. and J.S. requested and obtained the Fermi-LAT observations. T.N. requested and obtained the Swift observation. K.-L.L. analysed the Fermi-LAT, Swift X-ray telescope, AAVSO and VSNET observations. J.S. analysed the ARAS observations. B.D.M., I.V. and A.M.B. worked on the theoretical interpretation of the data. T.F. contributed to the distance and extinction estimations and provided useful data from V1324 Sco and V339 Del for meaningful comparisons. All authors discussed the results and commented on the final paper.

Competing interests

The authors declare no competing financial interests.

Additional information

Supplementary information is available for this paper at doi:10.1038/s41550-017-0222-1.

Correspondence and requests for materials should be addressed to K.-L.L. or B.D.M. or L.C.